Cobalt bis(dicarbollide) is a DNA-neutral pharmacophore

Krzysztof Fink*[,†,‡], Jakub Cebula[†,‡], Zdeněk Tošner[§], Mateusz Psurski[‖], Mariusz Uchman[‡], and Tomasz M. Goszczyński[†]

[†] Laboratory of Biomedical Chemistry, Hirszfeld Institute of Immunology and Experimental Therapy, Polish Academy of Sciences, 12 Rudolf Weigl St., 53-114 Wrocław, Poland

[‡] Department of Physical and Macromolecular Chemistry, Faculty of Science, Charles University, Hlavova 2030, 128 40 Prague 2, Czechia

[§] NMR Laboratory, Faculty of Science, Charles University, Hlavova 2030, 128 40 Prague 2, Czechia

[‖] Laboratory of Experimental Anticancer Therapy, Hirszfeld Institute of Immunology and Experimental Therapy, Polish Academy of Sciences, 12 Rudolf Weigl St., 53-114 Wrocław, Poland

Abstract

Cobalt bis(dicarbollide) (COSAN) is a metallacarborane used as a versatile pharmacophore to prepare biologically active hybrid organic–inorganic compounds or to improve the pharmacological properties of nucleosides, antisense oligonucleotides, and DNA intercalators. Despite these applications, COSAN interactions with nucleic acids remain unclear, limiting further advances in metallacarborane-based drug development. Although COSAN intercalates into DNA, COSAN-containing intercalators do not, and while COSAN shows low cytotoxicity, intercalators are often highly toxic. The present study aimed at comprehensively characterizing interactions between COSAN and DNA using a wide range of techniques, including UV–Vis absorption, circular (CD) and linear (LD) dichroism, nuclear magnetic resonance (NMR) spectroscopy, thermal denaturation, viscosity, differential scanning calorimetry (DSC), isothermal titration calorimetry (ITC), and equilibrium dialysis measurements. Our results showed that COSAN has no effect on DNA structure, length, stability, or hybridization, with no or only faint signs of COSAN binding to DNA. Moreover, DNA is not necessary for COSAN to induce cytotoxicity at high concentrations, as shown by *in vitro* experiments. These findings demonstrate that COSAN is a DNA-neutral pharmacophore, thus confirming the general safety and biocompatibility of metallacarboranes and opening up new opportunities for further developing metallacarborane-based drugs.

INTRODUCTION

Metallacarboranes are versatile platforms commonly used to develop bioactive compounds with potential therapeutic applications. [1,2] Their unusual cage-like structure enables us to arrange substituents and tailor molecular targets. [3-5] Additionally, metallacarboranes can induce favorable interactions with biomolecules through hydrogen and dihydrogen bonding, [6,7] ion-pairing, [8,9] hydrophobic interactions, [3,5,7] and chaotropic effects. [10] Among metallacarboranes, cobalt bis(dicarbollide) (COSAN) stands out for its properties. [11]

Amphiphilic COSAN self-assembles in aqueous solutions[12-17] and interacts with lipid membranes[10,18-22] and hydrophobic cavities of cyclodextrins or proteins. [3,5,10,23] COSAN can also cross cell membranes and accumulate intracellularly, including in the cell nucleus. [18,19,21] Furthermore, 3D aromaticity[24,25] and a single negative charge delocalized over 23 atoms[26] explain the exceptional thermal, chemical, and biological stability of this abiotic compound. [2,27] Combined, these properties have prompted advances in drug design and gene therapy, thus explaining the increasing popularity of COSAN in medicinal chemistry. [1,2]

As a pharmacophore, COSAN is commonly used to prepare biologically active hybrid organic–inorganic derivatives. [28] These COSAN derivatives are applied as boron neutron capture therapy (BNCT) [18,29], radioimaging and magnetic resonance imaging[30] probes, enzyme inhibitors[3,7], antimicrobial agents[11,31,32], and peptide modifiers[33-35] They are also widely conjugated to nucleosides[36,37], antisense oligonucleotides[38,39], and DNA intercalators[40] to improve their pharmacological properties. Given the increasing number and variety of COSAN applications in biosciences, the biological properties of COSAN derivatives must be judiciously characterized, particularly their interactions with biomacromolecules, including proteins, lipid membranes, and nucleic acids such as DNA.

DNA-binding molecules, including intercalators and groove binders, are usually positively charged. The main modes of reversible ligand binding to double-stranded DNA (dsDNA) are (i) intercalation between DNA base pairs, (ii) interactions with the DNA minor groove, (iii) interactions with the DNA major groove, and (iv) electrostatic interactions with the anionic sugar-phosphate backbone of DNA. [41] Classical intercalators have planar fused aromatic ring systems, which stack between base pairs in the intercalation complex. [42] Groove binding compounds have unfused aromatic ring systems with the conformation needed to fit into the helical curvature of DNA grooves.

Regardless of DNA-binding mode, strong interactions with DNA require an electrostatic component. Electrostatic interactions are especially important for DNA-binding nuclear proteins or polyamines, which bind to the major groove or sugar-phosphate backbone of DNA. But the structure of COSAN markedly differs from the structure of known DNA-binding molecules. COSAN has a bulky, globular, and rigid structure with delocalized negative charge. For comparison, Figure 1 shows the structures of COSAN, the intercalator ethidium bromide (EB), the minor groove-binder 4',6-diamidino-2-phenylindole (DAPI), and the major grove/backbone-binder spermine, a polyamine.

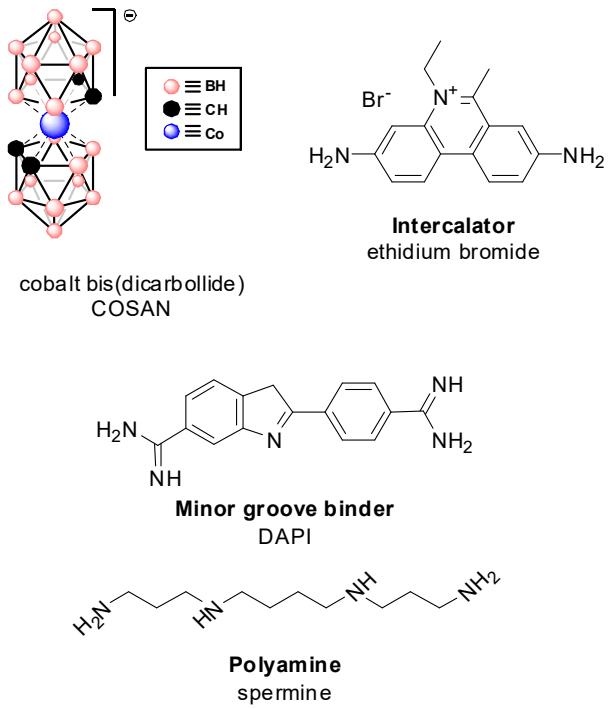

Figure 1. Structures of cobalt bis(dicarbollide), COSAN, and representative DNA-binding molecules: the intercalator ethidium bromide, the minor groove-binder 4',6-diamidino-2-phenylindole (DAPI), and the backbone-binder spermine, a polyamine.

Perhaps due to its unique structure, COSAN interactions with DNA remain, however, controversial. On the one hand, studies on interactions between COSAN and DNA have reported that this metallacarborane intercalates into DNA. [18,43] On the other hand, research on COSAN conjugated with the intercalator naphthalimide or with oligonucleotides have failed to support these claims. [38-40,44] In fact, COSAN conjugation to naphthalimide decreased its affinity to DNA and altered its binding mode to groove binding, as shown by minor changes in the DNA melting temperature and circular dichroism spectrum. [40] Furthermore, COSAN-containing oligonucleotides maintain their ability to hybridize with complementary strands, forming duplexes with structures similar to those of the corresponding COSAN-free duplexes. [38,39,44] COSAN also shows low toxicity to mammalian cells, [18,45,46] whereas intercalators are often highly toxic. In short, the data on COSAN-DNA interactions are still inconclusive.

Considering the above, we aimed at investigating the interaction between COSAN and DNA using a wide range of spectroscopic, calorimetric, and other physicochemical techniques, such as UV–Vis absorption spectroscopy, circular (CD) and linear (LD) dichroism, and nuclear magnetic resonance (NMR). In addition, we performed thermal denaturation, viscosity, differential scanning calorimetry (DSC), isothermal titration calorimetry (ITC), and equilibrium dialysis measurements. Adequately characterizing COSAN-DNA interactions is crucial for further advancing metallacarborane-based drug development and for addressing safety concerns because DNA-binding molecules often have associated mutagenic, cancerogenic, or teratogenic activity. This knowledge will facilitate the rational design of metallacarborane-based drugs and unveil their molecular mechanism of action, thereby overcoming current limitations to metallacarborane applications in medicinal chemistry. [47]

RESULTS

Spectral analysis of COSAN – DNA solutions

UV–Vis absorption spectroscopy is an effective method for studying small molecule interactions with DNA, irrespective of binding mode. Whether through intercalation, groove binding or external binding to the DNA backbone, these interactions with DNA should lead to changes in the absorption spectra of both the small molecule and DNA. [48-50] Figure 2A shows absorption spectra of free DNA from calf thymus (ctDNA) and ctDNA at increasing concentrations of COSAN ([COSAN]/[ctDNA(per base, pb)] ratios ranging from 0.125 to 1). Because the absorption band of COSAN overlaps with that of ctDNA, all measured spectra were adjusted to the corresponding concentration of COSAN. ctDNA has a single, broad absorption band, with an absorbance maximum at 258 nm. After adding COSAN, the absorption spectra of ctDNA remained unchanged.

COSAN has a strong absorption band at 282 nm (ε = 30,866 M^{-1} cm^{-1}, Figure S1A and B) and a weak absorption band at 448 nm (ε = 443.5 M^{-1} cm^{-1}, Figure S1C and D). The strong absorption band overlaps with the absorption band of DNA. Thus, to study the interaction between COSAN and DNA, we measured the absorbance of COSAN with increasing concentrations of DNA in the wavelength range of 380 – 600 nm. Figure 2B shows the absorption spectra of free COSAN and COSAN with increasing concentrations of ctDNA ([ctDNA(pb)]/[COSAN] ratios ranging from 0.25 to 1.5). We observed no changes in the absorption spectra of COSAN after adding DNA. Overall, these results indicate that no or only a very weak complex is formed between COSAN and ctDNA.

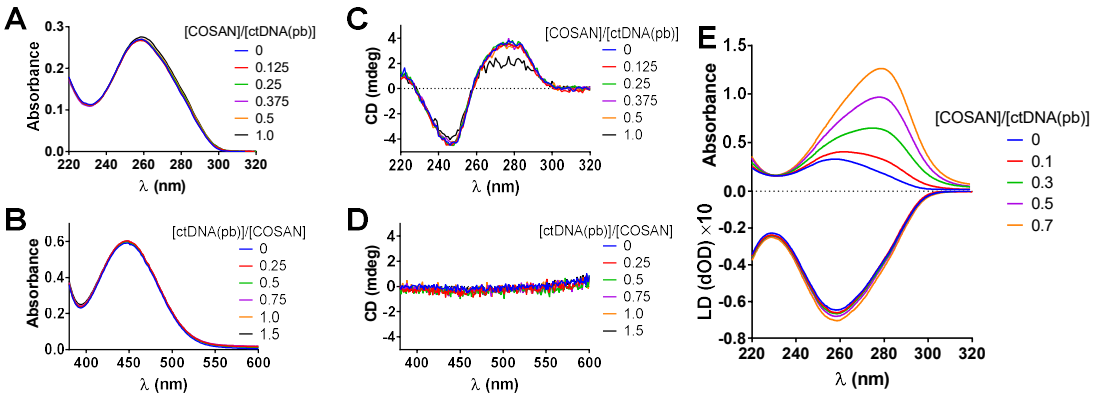

Figure 2. Absorption spectra of (**A**) ctDNA (0.4 mM (pb)) with increasing concentrations of COSAN (0 to 0.4 mM) and (**B**) COSAN (1.5 mM) with increasing concentrations of DNA (0 to 2.25 mM (pb)). Circular dichroism (CD) spectra of (**C**) ctDNA (0.4 mM (pb)) with increasing concentrations of COSAN (0 to 0.4 mM). (**D**) CD spectra of COSAN (1.5 mM) with increasing concentrations of ctDNA (0 to 2.25 mM (pb)). (**E**) Absorption and linear dichroism (LD) spectra of ctDNA (1.0 mM (pb)) with increasing concentrations of COSAN (0 to 0.7 mM). All spectra were measured in 20 mM phosphate buffer with 150 mM NaCl and 1 mM EDTA, pH 7.4.

Subsequently, we measured circular dichroism (CD) and linear dichroism (LD) spectra of DNA in the presence of COSAN. Both techniques provide information about DNA structural changes induced by ligand binding. [51] Figure 2C shows the CD spectra of ctDNA with COSAN ([COSAN]/[ctDNA(pb)] ratios ranging from 0 to 1).

The CD spectrum of ctDNA is characteristic of the right-handed B form and consists of a positive band at 275 nm due to base stacking and a negative band at 245 nm due to helicity. [52] Both bands are highly sensitive to the intercalation of small molecules with DNA. However, CD spectra of DNA show no or only very little alteration in electrostatic binding and minor groove binding. [53] At [COSAN]/[ctDNA(pb)] ratios ranging from 0.125 to 0.375, no changes were identified in the CD spectra. At a [COSAN]/[ctDNA(pb)] ratio of 0.5, the intensity of the positive band at 275 nm decreased. At a [COSAN]/[ctDNA(pb)] ratio of 1, the intensity of both the positive band at 275 nm and the negative band at 245 nm further decreased. These changes in the DNA CD spectrum may be explained by at least three reasons: (i) perturbation of the DNA structure, (ii) appearance of the induced CD (ICD) signal of COSAN, and (iii) quenching of the DNA CD signal by light absorption by COSAN. The first explanation is inconsistent with the results of UV–Vis absorption measurements because the perturbation of DNA structure would also entail changes in the DNA absorption spectrum.

To test the second hypothesis, we measured CD spectra in the wavelength range from 380 to 600 nm, where COSAN has a weak absorption band, which does not overlap with the DNA absorption band. Figure 2D shows the CD spectra of COSAN with ctDNA ([ctDNA(pb)]/[COSAN] ratios ranging from 0 to 1.5). Achiral molecules, such as COSAN, lack a CD spectrum, but upon binding to DNA, either through intercalation or minor-groove binding, they are in the chiral environment of DNA and thus acquire an ICD signal. [54] By contrast, in the presence of ctDNA, COSAN lacks an ICD signal. For this reason, we rejected the second hypothesis.

To test the third hypothesis, we conducted measurements using a double-cuvette system in which one cuvette (closer to the light source) contained various concentrations of free COSAN (0, 0.2, and 0.4 mM), and the second cuvette contained free ctDNA (0.4 mM (pb)) (Figure S2A and B). In that setup,

the light was first absorbed by the cuvette with COSAN and then passed through the cuvette with ctDNA, which allowed us to assess the COSAN light absorption effect on the ctDNA CD spectrum. We observed the same effect as in the original measurements, that is, a decreased intensity of the DNA CD bands (Figure S2C–E). These changes in the DNA CD spectrum resulted from DNA CD signal quenching caused by COSAN light absorption. Thus, our CD measurements show that COSAN does not affect the secondary structure of DNA.

Bulky molecules, such as COSAN, may have slow DNA-binding kinetics because they must overcome structural barriers and need extensive DNA unwinding. [55] Accordingly, we repeated the UV–Vis and CD measurements of ctDNA and ctDNA with COSAN ([COSAN]/[ctDNA(pb)] ratio from 0 to 0.5) after seven days of incubation at room temperature (Figure S3 and S4). Nevertheless, we observed no differences in either the UV–Vis or CD spectra of ctDNA after adding COSAN. These results indicate that COSAN does not interact with ctDNA.

LD spectroscopy measures the difference between the absorption of linearly polarized light travelling parallel and perpendicular to the orientation of a sample. CtDNA consists of dsDNA strands long enough to be oriented in the Couette flow and has a negative LD band in its absorbance region. In contrast, COSAN is a small molecule and is not oriented in the flow, thus lacking an LD signal. However, COSAN may be oriented in the flow along with DNA and acquire an LD signal by interacting with DNA either through intercalation or minor-grove binding. Although the absorbance spectra of COSAN and DNA overlap, COSAN clearly contributed to the absorbance spectra (Figure 2E).

The LD spectrum of free ctDNA shows a negative absorption band with a minimum at 258 nm, which indicates that the average orientation of the DNA bases was nearly perpendicular to the direction of flow (Figure 2E). The LD spectra of ctDNA with increasing concentrations of COSAN ([COSAN]/[ctDNA(pb)] = 0.1 to 0.7) show that the magnitude of the LD signal at 258 nm increases by approximately 9% at [COSAN]/[ctDNA(pb)] = 0.7, so adding COSAN slightly increases the orientation of DNA bases in the direction of flow. However, this effect is weak. To put this number into the context, for ethidium bromide (EB), the magnitude of the LD signal between free DNA and DNA with EB at a molar ratio of 0.1 increases by over 70%.[56] Furthermore, no LD signal was detected at 282 nm (COSAN absorbance region), which suggests that COSAN does not bind to ctDNA in a way that promotes its orientation in the direction of flow along with ctDNA. Overall, these LD measurements show that COSAN is not intercalated into DNA or bound to minor DNA grooves.

COSAN effect on DNA length, stability, and hybridization

The intercalation of small molecules into DNA separates DNA base pairs, lengthening the DNA, as shown by the increased viscosity of the DNA solution. [57] We measured the viscosity of a solution with a constant concentration of ctDNA (0.24 mM (pb)) at increasing COSAN concentrations (from 0 to 0.12 mM). The data were plotted as the $(\eta/\eta_0)^{1/3}$ function of the [COSAN]/[ctDNA(pb)] ratio, where η is the intrinsic viscosity of the solution containing ctDNA and COSAN, and η_0 is the intrinsic viscosity of the solution containing free ctDNA (Figure 3A). At [COSAN]/[ctDNA(pb)] ratios ranging from 0.083 to 0.25, $(\eta/\eta_0)^{1/3}$ remained unchanged and close to 1. At [COSAN]/[ctDNA(pb)] ratios ranging from 0.25 to 0.417, $(\eta/\eta_0)^{1/3}$ slightly decreased to 0.96, albeit nonsignificantly. At a [COSAN]/[ctDNA(pb)] ratio of 0.5, the trend reversed, and $(\eta/\eta_0)^{1/3}$ returned to approximately 1. Overall, we did not detect any significant changes in DNA viscosity after adding COSAN. These findings also indicate that COSAN does not intercalate into DNA.

The COSAN effect on the stability of the dsDNA helix was determined by thermal denaturation whereby dsDNA separates into two single strands through DNA melting by increasing the temperature. The temperature at which half of the DNA strands are separated is termed the melting temperature (T_m).

Intercalators stabilize the dsDNA helix, which increases T_m, whereas molecules that interact with DNA in a non-intercalative mode usually do not change the T_m of DNA. [57] . The intercalation of such a bulky molecule as COSAN should cause structural changes in DNA, affecting its stability, through constructive or destructive effects, and changing the DNA melting temperature.

By differential scanning calorimetry (DSC), we assessed COSAN effects on ctDNA melting transitions. Figure 3B shows DSC thermograms of free ctDNA and ctDNA with COSAN at a [COSAN]/ctDNA(bp)] ratio of 0.13. As expected for genomic DNA, ctDNA has a complex melting profile with several transitions because ctDNA consists of long strands with many domains, which melt independently. [58] The thermogram of ctDNA with COSAN shows the same shape and position as the melting profile of free ctDNA. The values of the maximum temperature of the molar heat capacity curve (T_{max}) are the same for both free ctDNA and ctDNA with COSAN (Figure 3B). Furthermore, by analyzing the thermograms using Gaussian models in the NanoAnalyze program, we deconvoluted both melting profiles into five separate transitions (Figure S6). With COSAN, the melting temperatures (T_m) of each transition showed no significant differences with free ctDNA (Table S1). Based on these results, COSAN most likely does not affect the melting transitions of DNA and, thus, should not intercalate into DNA.

DNA thermal melting can also be analyzed by measuring absorbance at 260 nm in a temperature gradient. In this study, we used a short oligonucleotide (oligoDNA) with a palindromic sequence of 5'-CGCGAATTCGCG-3', which forms B-form dsDNA, [59] for two reasons. First, oligoDNA has a lower T_m than ctDNA, which enables measurements in a temperature gradient below the boiling temperature of water. Second, in contrast to long ctDNA strands, short oligoDNA strands can reform the dsDNA structure after heating and cooling to room temperature through a process known as DNA annealing. This ability of short oligoDNA strands to anneal allowed us to assess COSAN effects not only on DNA melting but also on the hybridization of two complementary ssDNA molecules into the dsDNA helix.

Figure 3C shows the normalized absorbance at 260 nm of free oligoDNA and oligoDNA with COSAN ([COSAN]/[oligoDNA (pb)] = 0.2) in a temperature range from 25 to 90 °C. The calculated T_m of free oligoDNA was 54.3 $\pm$ 0.4 °C. Adding COSAN did not affect the T_m of the oligoDNA (54.1 ± 0.3 °C), which indicates that COSAN does not intercalate into DNA. Figure 3D shows CD spectra of oligoDNA with COSAN ([COSAN]/[oligoDNA (pb)] = 0.2) before and after heating and cooling back to 25 °C. The CD spectra of oligoDNA and oligoDNA with COSAN, measured before heating, are similar and indicate that COSAN does not affect the structure of DNA, in line with CD measurements of ctDNA with COSAN. No differences were found between the CD spectra of free oligoDNA or oligoDNA with COSAN, measured before and after heating. These results demonstrate that oligoDNA can return to the helical, ds B-form after melting despite the presence of COSAN (Figure 3D and E).

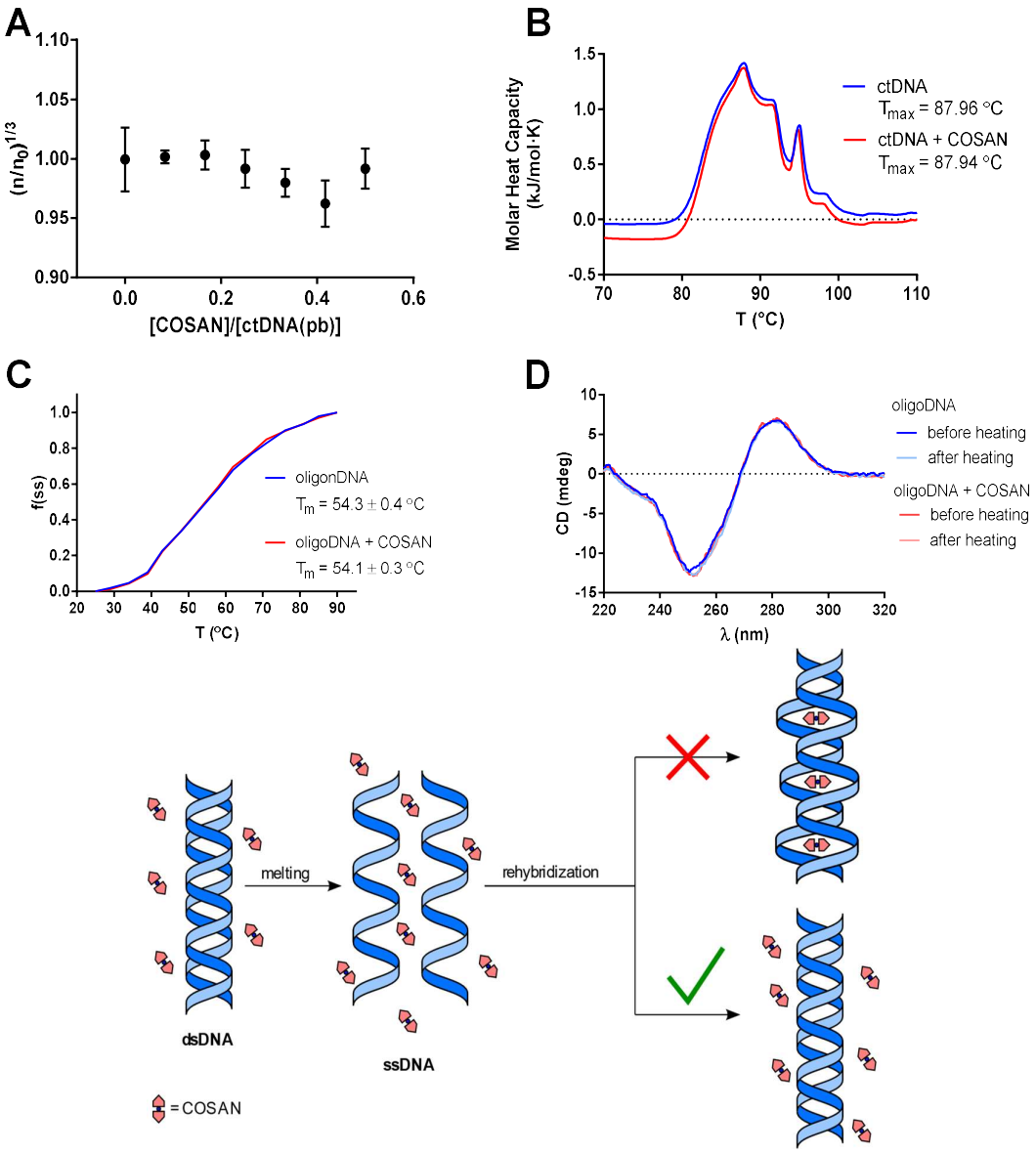

Figure 3. COSAN does not affect DNA length, melting, and rehybridization. (**A**) Relative intrinsic viscosity $(\eta/\eta_0)^{1/3}$ of ctDNA (0.24 mM (pb)) at increasing concentrations of COSAN (ranging from 0 to 0.12 mM). (**B**) DSC thermograms with melting curves of free ctDNA (3.0 mM (pb)) and ctDNA with COSAN (0.4 mM) at temperatures ranging from 20 to 120 °C, 1 °C/min heating rate, 3 atm pressure. (**C**) Melting profiles of oligoDNA (5'-CGCGAATTCGCG-3') (0.05 mM (pb)) with (oligoDNA + COSAN) and without (oligoDNA) 0.01 mM COSAN in a temperature range from 25 to 90 °C. f(ss) = $(A-A_0)/(A_f-A_0)$, where A is the absorption at 260 nm at temperatures between 25 and 90 °C, A_0 is the absorption at 260 nm at 25 °C, and A_f is the absorption at 260 nm at 90 °C. (**D**) Circular dichroism (CD) spectra of 0.05 mM (pb) oligoDNA (5'-CGCGAATTCGCG-3') with (oligoDNA + COSAN) and without (oligoDNA) 0.01 mM COSAN at 25 °C before and after heating to 90 °C and cooling back to 25 °C. (**E**) Schematic representation of dsDNA melting into ssDNA and rehybridization of ssDNA into dsDNA in the presence of COSAN. DSC and viscosity were measured in 20 mM phosphate buffer with 150 mM NaCl and 1 mM EDTA, pH 7.4. Absorption and CD spectra of the oligoDNA were measured in 10 mM phosphate buffer with 100 mM NaCl and 0.1 mM EDTA, pH 7.0.

COSAN–DNA binding

As shown above, COSAN cannot intercalate into DNA or bind to the DNA minor groove. However, other modes of interaction remain possible. To detect the formation of COSAN-DNA complexes regardless of their mode of interaction, we used three other methods, namely ITC, equilibrium dialysis, and NMR.

The thermodynamic profile of the interaction between COSAN and DNA was assessed by ITC. For ITC, COSAN (5.0 mM) was titrated into 1.0 mM (pb) ctDNA solution. The resulting ITC profile was corrected by subtracting the corresponding dilution heats derived from COSAN injections into the buffer (Figure 4A). The plot of the measured enthalpy values as a function of the [COSAN]/[ctDNA(pb)] ratio shows a random distribution of enthalpy values around zero kJ/mol (Figure 4B). The mean enthalpy per injection was -0.11315 $\pm$ 0.18784 kJ/mol, which shows that COSAN titration into ctDNA shows no heat effect, thus indicating that COSAN does not interact with DNA.

The results of the equilibrium dialysis experiments are shown in Figure 4C, where the percentage of COSAN (0.05 mM) bound (%bound) to ctDNA is plotted as a function of the [ctDNA(pb)]/[COSAN] ratio (0–20). At [ctDNA(pb)]/[COSAN] ratios of 0.2, 1, and 4, approximately 0% of COSAN is bound to ctDNA. At a [ctDNA(pb)]/[COSAN] ratio of 20, the amount of bound COSAN increased to 12.8%, but this result was not significant (one-way ANOVA, *p*-value = 0.1228). Nevertheless, this small fraction of COSAN bound to DNA suggests a weak interaction between COSAN and DNA. But COSAN may alternatively interact with residual proteins remaining in solution after ctDNA purification. The certificate of ctDNA analysis used in this study states that the product contains 1% of proteins (Figure S19). Since COSAN and its derivatives showed a high affinity to proteins, COSAN might have bound to proteins in the DNA sample, thereby explaining its retention in the DNA-containing chamber. As a positive control, we conducted equilibrium dialysis of COSAN with human serum albumin (HSA). COSAN has a high affinity to serum albumin, [23] as confirmed in the equilibrium dialysis experiment, where the percentage of COSAN bound to HSA was 100%.

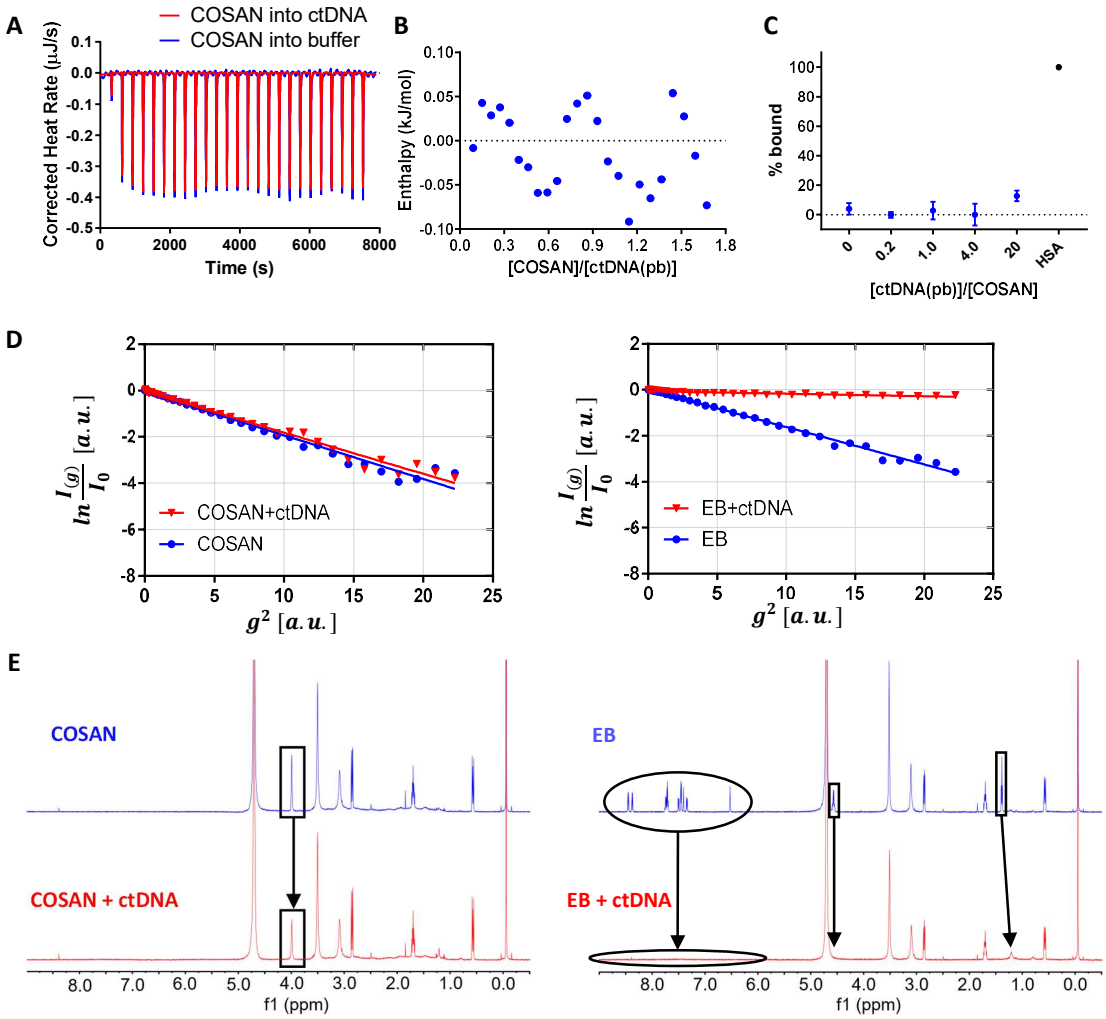

Figure 4. (**A**) Thermograms of COSAN titrations (5.0 mM) into ctDNA (1.0 mM (pb)) (COSAN into ctDNA) or the buffer (COSAN into buffer). (**B**) Enthalpograms of titrations of COSAN (5.0 mM) into ctDNA (1.0 mM (pb)) after subtracting the blank titration. (**C**) Plot of the percentage of COSAN (0.05 mM) bound to ctDNA as a function of [ctDNA(pb)]/[COSAN] ratio (0, 0.2, 1.0, and 20) based on equilibrium dialysis. The percentage of COSAN (0.05 mM) bound to human serum albumin (HSA, 0.05 mM) served as a positive control. All measurements were conducted in 20 mM phosphate buffer with 150 mM NaCl and 1 mM EDTA, pH 7.4. (**D**) Graphical representation of DOSY decay of COSAN (0.6 mM) and EB (0.6 mM), with and without DNA (3.0 mM (pb)). The results were calculated from the Stejskal-Tannor equation. (**E**) H^1 NMR spectra of COSAN (0.6 mM) and EB (0.6 mM) with (bottom) and without (top) ctDNA (3.0 mM (pb)). Peaks representing COSAN and EB are marked on the spectra. The remaining peaks belong to residual water, EDTA, and DSS. Detailed spectra are available in Figures S20-36.

Lastly, we used NMR-based methods to study interactions between DNA and COSAN, i.e., diffusion-ordered spectroscopy (DOSY) and ^{1}H NMR.[60] Ethidium bromide (EB), a model intercalator, was used as a control. Either COSAN or EB binding to ctDNA should decrease the diffusion rate of the ligand because ctDNA is significantly larger and slower. The measurements were conducted at concentration ratios of COSAN/ctDNA(pb) spanning from 1:1 to 1:15. The DOSY results show that the diffusion coefficients (D) of COSAN remained virtually unchanged in all samples with and without ctDNA, but the diffusion coefficient of EB was an order of magnitude smaller with DNA than without DNA, indicating that EB bound to ctDNA (Table 1, Figure 4D).

Table 1. Diffusion coefficients and integrations of H^1 NMR signals of COSAN and ethidium bromide (EB) measured with and without ctDNA

Sample	c_t [mM]	c_m [mM][b]	D $[10^{-10}\ m^2s^{-1}]$
COSAN	0.2	0.22	4.92
	0.6	0.59	4.95
	3	2.90	5.05
COSAN+ctDNA[a]	0.2	0.20	5.21
	0.6	0.65	5.31
	3	2.97	5.18
EB	0.6	0.61	4.38
EB+ctDNA[a]	0.6	0.29	< 0.1

[a] The concentration of ctDNA was kept constant at 3 mM (pb). [b] The COSAN data were calculated from CH protons, and the EB data were calculated from CH3 signals. Abbreviations: D – absolute diffusion coefficient, c_t – theoretical concentration of either COSAN or EB, c_m – concentration of either COSAN or EB measured by H^1 NMR.

DOSY experiments cannot completely rule out binding because the lack of differences in COSAN diffusion coefficients might have resulted from the rapid exchange between bound and unbound fractions of COSAN. To exclude this possibility, ^{1}H NMR spectra were investigated using an internal standard. COSAN signals and their integrations in samples with and without DNA remained within the experimental error, with no significant shifts (Table 1 and Figure 4E). Conversely, EB samples showed clear differences between spectra with and without DNA. In the presence of DNA, most EB signals disappeared, except for the signal of the very mobile CH3 group, which was weaker and shifted. These results confirm the lack of binding between COSAN and DNA.

COSAN toxicity to anuclear and nuclear cells

Previous studies have shown that COSAN has moderate to low toxicity toward eukaryotic cells. [18,45,46] However, the mechanism of this toxicity is still obscure. To assess whether COSAN toxicity depends on its interaction with DNA, we conducted *in vitro* experiments on six cell lines and red blood cells (RBCs) because mature RBCs lack a nucleus (anuclear) and DNA but are packed with hemoglobin. By *in vitro* hemolysis, we determined COSAN toxicity to RBCs by measuring hemoglobin release due to RBC membrane disruption. COSAN showed moderate hemolytic activity, with a concentration at 50% hemolysis (EC_{50}) of 100.5 µM (Table 2). Accordingly, COSAN may have a purely membranolytic activity towards cells without interacting with DNA.

COSAN toxicity to nuclear cells matched its hemolytic toxicity, with COSAN inhibiting 50% of cell proliferation (IC_{50}) in the concentration range from 29.3 to 106.6 µM depending on the cell line (Table 2, Figure S38). In other words, COSAN affects nuclear cell viability at concentrations similar to those that induce RBC membrane disruption. Although these results suggest that COSAN toxicity to nuclear cells also involves cell membrane disruption, further studies must be conducted to confirm this hypothesis.

Table 2. Hemolytic and cytotoxic activity of COSAN

Compound	Hemolysis EC_{50} (μM)	Cytotoxicity IC_{50} (μM)					
		MCF10A	BALB/3T3	A549	MV-4-11	PC-3	UM-UC-3
COSAN	100.5 (95.5–105)	67.0 (61.4–74.4)	31.1 (25.6–37.1)	44.9 (36.3–55.4)	37.7 (29.3–49.6)	29.3 (16.4–202)	106.6 (97.2–117)

Abbreviations: EC_{50} – half maximal effective concentration of hemolysis, IC_{50} – half maximal inhibitory concentration of proliferation; the values of the 95% confidence interval (95% CI) are presented in brackets.

DISCUSSION

The bulky structure of COSAN contrast with the structures of classical intercalators or groove binders. COSAN has a peanut-shaped, 11-Å-long, and 6-Å-wide structure[61], whereas the distance between adjacent base pairs in the B-form DNA helix is 3.6 Å and the minor groove of DNA is 4.8 Å wide. Although, DNA is flexible enough to accommodate bulky molecules (e.g., DNA can unwind to enable steroids to intercalate) [62], the DNA structure shows no changes in UV-Vis, CD, LD, and viscosity measurements suggesting COSAN binding.

In addition to the discordant structure, COSAN provides almost no opportunities for the formation of new bonds with DNA. Classical intercalators interact with DNA base pairs through their π-electron systems, forming new π-π stacking bonds. These bonds stabilize the dsDNA structure and increase the DNA melting temperature (T_m). But while COSAN is an aromatic molecule, its 3D aromaticity is delocalized over σ-bonds. [26] As such, COSAN lacks the π-electron system of classical intercalators and cannot form new stacking bonds with adjacent DNA base pairs.

Minor and major groove binders interact with DNA through hydrogen bonds and van der Waals interactions. [63] COSAN has C–H groups, which can form hydrogen bonds with N and O H-bond acceptors in DNA bases in minor and major grooves. [64] However, these hydrogen bonds are much weaker than classical hydrogen bonds. Additionally, B–H groups in COSAN can participate in dihydrogen bonds with proton donors, such as the N–H groups of DNA bases. [6] Dihydrogen bonds are also weaker than classical hydrogen bonds, and DNA grooves have fewer partners for dihydrogen bonding than for classical hydrogen bonding: the minor groove has only one N–H group (guanine), whereas the major groove has two N–H groups (adenine and cytosine) available for dihydrogen bonding.

Lastly, external binding involves electrostatic interactions between DNA anionic sugar-phosphate backbone and positively charged compounds. COSAN is an anion with a single delocalized charge. Therefore, COSAN is unlikely to interact with the DNA backbone due to electrostatic repulsion.

These considerations agree with our experimental findings. The melting temperature of DNA does not change in the presence of COSAN, showing that COSAN has no significant effect on the stability of DNA strands. Furthermore, ITC, equilibrium dialysis and NMR measurements showed no binding between COSAN and DNA. In equilibrium dialysis, only at a high [ctDNA(pb)]/[COSAN] ratio of 20 did a small fraction of COSAN bind to DNA, which might have even been an artifact of interactions between COSAN and residual proteins present in the DNA sample. And intercalation or minor groove binding would have placed COSAN in the chiral environment of DNA and align this molecule with DNA in the Couette flow, which we did not observe in CD and LD measurements, respectively.

In the absence of any evidence of COSAN binding to dsDNA, we assessed COSAN effects on ssDNA hybridization. COSAN should more easily form complexes with ssDNA than with dsDNA because 1) ssDNA has a lower surface charge density than dsDNA, weakening the repulsive Coulombic forces between COSAN and DNA, 2) ssDNA is more flexible than dsDNA, facilitating the conformational

adaptation of DNA to COSAN, and 3) ssDNA has exposed nucleobases, providing additional potential partners for COSAN binding. Our CD measurements of oligoDNA before and after its thermal melting showed that COSAN does not interfere with the annealing of two complementary DNA single strands. Therefore, COSAN does not significantly interact with ssDNA, in line with previous studies on metallacarborane-modified oligonucleotides, which formed complexes with complementary nucleic acid strands. [36,38,39,44,65]

Our findings indicate that COSAN and, most likely, other metallacarboranes are poor pharmacophores for nucleic acid-binding drugs. Instead, COSAN should be used to target nucleic acid-binding proteins – such as transcription factors, histones, topoisomerases, polymerases, or DNA methyltransferases – which are components of biomolecular condensates and participate in many vital cellular processes. [66] Because the dysfunction of these proteins has been implicated in many diseases, including cancer, [67] small molecules capable of modulating their activity have a high therapeutic potential.

The obstacle to developing such therapeutics is the unconventional structure of nucleic acid-binding domains in these proteins. Unlike the enclosed binding pockets of enzymes or receptor active sites, nucleic acid-binding domains have convex, exposed, and highly positively charged interfaces. [68] These properties complicate the development of small-molecule inhibitors of nucleic acid-binding proteins. For this reason, these proteins have long been deemed 'undruggable'.

Considering the nonplanar structure of metallacarboranes, which enables the 3D arrangement of substituents, as well as their high interaction capacity and their affinity to large, flexible, and open enzyme active sites, [3,5,28] metallacarborane-based compounds may be well suited to target nucleic acid-binding proteins. Furthermore, in contrast to other bulky scaffolds, such as C60 fullerenes or carbon nanotubes, [69] metallacarboranes are indifferent to DNA, enabling selective protein binding. No such metallacarborane-based compounds are known yet, so further studies must be conducted to test this hypothesis.

In addition to our physicochemical results, we showed that COSAN cytotoxicity is independent of DNA. COSAN was as toxic to nuclear cells as to red blood cells (RBCs) without a cell nucleus or organelles. The membranolytic effect of COSAN on RBCs suggests that COSAN cytotoxicity is more likely explained by its interactions with cell membranes than by interactions with nucleic acids. Given the affinity of COSAN and its derivatives to proteins, its interactions with vital cellular proteins should also be analyzed in depth to better understand its cytotoxic effects.

CONCLUSIONS

DNA is a highly flexible molecule with the ability to accommodate molecules with various shapes and sizes. From a purely spatial point of view, COSAN could form complexes with DNA either through intercalation or groove binding, albeit requiring major structural changes in DNA. However, COSAN is unable to offset such structural changes by forming new bonds. Additionally, regardless of DNA-binding mode, ligand interactions with DNA usually include an electrostatic component between the cationic ligand and anionic DNA, which anionic COSAN cannot provide. COSAN has no effect on DNA structure, length, stability, or hybridization, and DNA, in turn, does not affect the absorption spectrum or diffusion coefficient of COSAN or induce CD or LD signals. COSAN titration into DNA has no heat effects. Based on theoretical considerations and on our experimental results, COSAN cannot form complexes with DNA, and DNA is not necessary for COSAN to induce toxicity, which is most likely protein- or cell membrane-dependent. In conclusion, COSAN is DNA-neutral pharmacophore without significant interactions with DNA, thus confirming the general safety and biocompatibility of metallacarboranes.

Author information

Corresponding author

E-mail: krzysztof.fink@hirszfeld.pl

ORCID

Krzysztof Fink: 0000-0002-1238-9653

Jakub Cebula: 0000-0002-7603-611X

Zdeněk Tošner: 0000-0003-2741-9154

Mateusz Psurski: 0000-0001-8866-7149

Mariusz Uchman: 0000-0002-2564-1985

Tomasz M. Goszczyński: 0000-0002-9995-3260

Notes

The authors declare no competing financial interest.

Acknowledgments

K.F. and T.M.G. would like to acknowledge the financial support of the National Science Centre, Poland, grant no. 2019/32/C/NZ7/00510 and 2016/23/D/NZ1/02611. J.C. would like to acknowledge the financial support of the Polish National Agency for Academic Exchange, grant no. PPN/STA/2021/1/00023. The authors thank Carlos V. Melo for editing the manuscript.

REFERENCES

1 Gabel, D. Boron clusters in medicinal chemistry: Perspectives and problems. *Pure Appl. Chem.* **87**, 173-179 (2015). https://doi.org:10.1515/pac-2014-1007

2 Lesnikowski, Z. J. Challenges and opportunities for the application of boron clusters in drug design. *J. Med. Chem.* **59**, 7738-7758 (2016). https://doi.org:10.1021/acs.jmedchem.5b01932

3 Gruner, B. *et al.* Metallacarborane sulfamides: Unconventional, specific, and highly selective inhibitors of carbonic anhydrase IX. *J. Med. Chem.* **62**, 9560-9575 (2019). https://doi.org:10.1021/acs.jmedchem.9b00945

4 Gruner, B. *et al.* Cobalt bis(dicarbollide) alkylsulfonamides: Potent and highly selective inhibitors of tumor specific carbonic anhydrase IX. *ChemPlusChem* **86**, 350-351 (2021). https://doi.org:10.1002/cplu.202000717

5 Cigler, P. *et al.* From nonpeptide toward noncarbon protease inhibitors: Metallacarboranes as specific and potent inhibitors of HIV protease. *Proc. Natl. Acad. Sci. U. S. A.* **102**, 15394-15399 (2005). https://doi.org:10.1073/pnas.0507577102

6 Fanfrlik, J., Lepsik, M., Horinek, D., Havlas, Z. & Hobza, P. Interaction of carboranes with biomolecules: Formation of dihydrogen bonds. *ChemPhysChem* **7**, 1100-1105 (2006). https://doi.org:10.1002/cphc.200500648

7 Kozisek, M. *et al.* Inorganic polyhedral metallacarborane inhibitors of HIV protease: A new approach to overcoming antiviral resistance. *J. Med. Chem.* **51**, 4839-4843 (2008). https://doi.org:10.1021/jm8002334

8 Plesek, J. *et al.* Potential uses of metallocarborane sandwich anions for analysis, characterization and isolation of various cations and organic-bases. *Collect. Czech. Chem. Commun.* **49**, 2776-2789 (1984). https://doi.org:DOI 10.1135/cccc19842776

9 Stoica, A. I., Vinas, C. & Teixidor, F. Cobaltabisdicarbollide anion receptor for enantiomer-selective membrane electrodes. *Chem. Commun.*, 4988-4990 (2009). https://doi.org:10.1039/b910645f

10 Assaf, K. I. *et al.* High-affinity binding of metallacarborane cobalt bis(dicarbollide) anions to cyclodextrins and application to membrane translocation. *J. Org. Chem.* **84**, 11790-11798 (2019). https://doi.org:10.1021/acs.joc.9b01688

11 Fink, K. & Uchman, M. Boron cluster compounds as new chemical leads for antimicrobial therapy. *Coord. Chem. Rev.* **431** (2021). https://doi.org:10.1016/J.Ccr.2020.213684

12 Matejicek, P., Cigler, P., Prochazka, K. & Kral, V. Molecular assembly of metallacarboranes in water: Light scattering and microscopy study. *Langmuir* **22**, 575-581 (2006). https://doi.org:10.1021/la052201s

13 Fernandez-Alvarez, R., Dordovic, V., Uchman, M. & Matejicek, P. Amphiphiles without head-and-tail design: Nanostructures based on the self-assembly of anionic boron cluster compounds. *Langmuir* **34**, 3541-3554 (2018). https://doi.org:10.1021/acs.langmuir.7b03306

14 Uchman, M., Abrikosov, A. I., Lepsik, M., Lund, M. & Matejicek, P. Micellization: Nonclassical hydrophobic effect in micellization: Molecular arrangement of non-amphiphilic structures. *Adv. Theory Simul.* **1**, 1870003 (2018).

15 Dordovic, V. *et al.* Stealth amphiphiles: Self-assembly of polyhedral boron clusters. *Langmuir* **32**, 6713-6722 (2016). https://doi.org:10.1021/acs.langmuir.6b01995

16 Uchman, M., Dordovic, V., Tosner, Z. & Matejicek, P. Classical amphiphilic behavior of nonclassical amphiphiles: A comparison of metallacarborane self-assembly with SDS micellization. *Angew. Chem. Int. Ed.* **54**, 14113-14117 (2015). https://doi.org:10.1002/anie.201506545

17 Malaspina, D. C., Vinas, C., Teixidor, F. & Faraudo, J. Atomistic simulations of COSAN: Amphiphiles without a head-and-tail design display "head and tail" surfactant behavior. *Angew. Chem. Int. Ed.* **59**, 3088-3092 (2020). https://doi.org:10.1002/anie.201913257

18 Fuentes, I. *et al.* Metallacarboranes on the road to anticancer therapies: Cellular uptake, DNA interaction, and biological evaluation of cobaltabisdicarbollide $[COSAN]^-$. *Chemistry* **24**, 17239-17254 (2018). https://doi.org:10.1002/chem.201803178

19 Tarres, M. *et al.* Biological interaction of living cells with COSAN-based synthetic vesicles. *Sci. Rep.* **5** (2015). https://doi.org:10.1038/Srep07804

20 Verdia-Baguena, C. *et al.* Amphiphilic COSAN and I2-COSAN crossing synthetic lipid membranes: Planar bilayers and liposomes. *Chem. Commun.* **50**, 6700-6703 (2014). https://doi.org:10.1039/c4cc01283f

21 Tarres, M., Canetta, E., Vinas, C., Teixidor, F. & Harwood, A. J. Imaging in living cells using vB-H Raman spectroscopy: Monitoring COSAN uptake. *Chem. Commun.* **50**, 3370-3372 (2014). https://doi.org:10.1039/c3cc49658a

22 Uchman, M. *et al.* Interaction of fluorescently substituted metallacarboranes with cyclodextrins and phospholipid bilayers: Fluorescence and light scattering study. *Langmuir* **26**, 6268-6275 (2010). https://doi.org:10.1021/la904047k

23 Goszczynski, T. M., Fink, K., Kowalski, K., Lesnikowski, Z. J. & Boratynski, J. Interactions of boron clusters and their derivatives with serum albumin. *Sci. Rep.* **7**, 9800 (2017). https://doi.org:10.1038/s41598-017-10314-0

24 King, R. B. Three-dimensional aromaticity in polyhedral boranes and related molecules. *Chem. Rev.* **101**, 1119-1152 (2001). https://doi.org:10.1021/cr000442t

25 Poater, J., Sola, M., Vinas, C. & Teixidor, F. π aromaticity and three-dimensional aromaticity: two sides of the same coin? *Angew. Chem. Int. Ed.* **53**, 12191-12195 (2014). https://doi.org:10.1002/anie.201407359

26 Farras, P. *et al.* Metallacarboranes and their interactions: Theoretical insights and their applicability. *Chem. Soc. Rev.* **41**, 3445-3463 (2012). https://doi.org:10.1039/c2cs15338f

27 Sivaev, I. B., Starikova, Z. A., Sjoberg, S. & Bregadze, V. I. Synthesis of functional derivatives of the [3,3'-Co(1,2-$C_2B_2H_{11})_2]^-$ anion. *J. Organomet. Chem.* **649**, 1-8 (2002). https://doi.org:10.1016/S0022-328x(01)01352-3

28 Meggers, E. From conventional to unusual enzyme inhibitor scaffolds: The quest for target specificity. *Angew. Chem. Int. Ed.* **50**, 2442-2448 (2011). https://doi.org:10.1002/anie.201005673

29 Nuez-Martinez, M. *et al.* Synchrotron-based Fourier-Transform Infrared Micro-Spectroscopy (SR-FTIRM) fingerprint of the small anionic molecule cobaltabis(dicarbollide) uptake in glioma stem cells. *Int. J. Mol. Sci.* **22** (2021). https://doi.org:10.3390/ijms22189937

30 Hawthorne, M. F. & Maderna, A. Applications of radiolabeled boron clusters to the diagnosis and treatment of cancer. *Chem. Rev.* **99**, 3421-3434 (1999). https://doi.org:10.1021/cr980442h

31 Kubinski, K. *et al.* Metallacarborane derivatives as innovative anti-candida albicans agents. *J. Med. Chem.* **65**, 13935–13945 (2022). https://doi.org:10.1021/acs.jmedchem.2c01167

32 Bennour, I. *et al.* Water soluble organometallic small molecules as promising antibacterial agents: Synthesis, physical-chemical properties and biological evaluation to tackle bacterial infections. *Dalton Trans.* **51**, 7188-7209 (2022). https://doi.org:10.1039/d2dt01015a

33 Fink, K., Boratynski, J., Paprocka, M. & Goszczynski, T. M. Metallacarboranes as a tool for enhancing the activity of therapeutic peptides. *Ann. N. Y. Acad. Sci.* **1457**, 128-141 (2019). https://doi.org:10.1111/nyas.14201

34 Fink, K., Kobak, K., Kasztura, M., Boratynski, J. & Goszczynski, T. M. Synthesis and biological activity of thymosin β4-anionic boron cluster conjugates. *Bioconjug. Chem.* **29**, 3509-3515 (2018). https://doi.org:10.1021/acs.bioconjchem.8b00646

35 Frank, R., Ahrens, V. M., Boehnke, S., Beck-Sickinger, A. G. & Hey-Hawkins, E. Charge-compensated metallacarborane building blocks for conjugation with peptides. *ChemBioChem* **17**, 308-317 (2016). https://doi.org:10.1002/cbic.201500569

36 Olejniczak, A. B., Plesek, J., Kriz, O. & Lesnikowski, Z. J. A nucleoside conjugate containing a metallacarborane group and its incorporation into a DNA oligonucleotide. *Angew. Chem. Int. Ed.* **42**, 5740-5743 (2003). https://doi.org:10.1002/anie.200352505

37 Lesnikowski, Z. J. *et al.* Towards new boron carriers for boron neutron capture therapy: Metallacarboranes and their nucleoside conjugates. *Bioorg. Med. Chem.* **13**, 4168-4175 (2005). https://doi.org:10.1016/j.bmc.2005.04.042

38 Kaniowski, D. *et al.* High boron-loaded DNA-oligomers as potential boron neutron capture therapy and antisense oligonucleotide dual-action anticancer agents. *Molecules* **22** (2017). https://doi.org:10.3390/molecules22091393

39 Ebenryter-Olbinska, K. *et al.* Versatile method for the site-specific modification of DNA with boron clusters: Anti-epidermal growth factor receptor (EGFR) antisense oligonucleotide case. *Chem. Eur. J.* **23**, 16535-16546 (2017). https://doi.org:10.1002/chem.201702957

40 Nekvinda, J. *et al.* Synthesis of naphthalimide-carborane and metallacarborane conjugates: Anticancer activity, DNA binding ability. *Bioorg. Chem.* **94**, 103432 (2020). https://doi.org:10.1016/j.bioorg.2019.103432

41 Strekowski, L. & Wilson, B. Noncovalent interactions with DNA: An overview. *Mutat. Res.* **623**, 3-13 (2007). https://doi.org:10.1016/j.mrfmmm.2007.03.008

42 Strekowski, L. & Wilson, B. Noncovalent interactions with DNA: An overview. *Mutat. Res. Fundam. Mol. Mech. Mutagen.* **623**, 3-13 (2007). https://doi.org:10.1016/j.mrfmmm.2007.03.008

43 Garcia-Mendiola, T. *et al.* Metallacarboranes as tunable redox potential electrochemical indicators for screening of gene mutation. *Chem. Sci.* **7**, 5786-5797 (2016). https://doi.org:10.1039/c6sc01567k

44 Kaniowski, D., Kulik, K., Suwara, J., Ebenryter-Olbinska, K. & Nawrot, B. Boron clusters as enhancers of RNase H activity in the smart strategy of gene silencing by antisense oligonucleotides. *Int. J. Mol. Sci.* **23** (2022). https://doi.org:10.3390/Ijms232012190

45 Tarres, M. *et al.* Biological interaction of living cells with COSAN-based synthetic vesicles. *Sci. Rep.* **5**, 7804 (2015). https://doi.org:10.1038/srep07804

46 Martinez, R. & Chacon-Garcia, L. The search of DNA-intercalators as antitumoral drugs: What it worked and what did not work. *Curr. Med. Chem.* **12**, 127-151 (2005). https://doi.org:http://dx.doi.org/10.2174/0929867053363414

47 Gozzi, M., Schwarze, B. & Hey-Hawkins, E. Preparing (metalla)carboranes for nanomedicine. *ChemMedChem* **16**, 1533-1565 (2021). https://doi.org:10.1002/cmdc.202000983

48 Zhang, L. Z. & Tang, G. Q. The binding properties of photosensitizer methylene blue to herring sperm DNA: A spectroscopic study. *J. Photochem. Photobiol. B, Biol.* **74**, 119-125 (2004). https://doi.org:10.1016/j.jphotobiol.2004.03.005

49 Ganeshpandian, M. *et al.* Mixed ligand copper(II) complexes of 2,9-dimethyl-1,10-phenanthroline: Tridentate 3N primary ligands determine DNA binding and cleavage and cytotoxicity. *J. Inorg. Biochem.* **140**, 202-212 (2014). https://doi.org:10.1016/j.jinorgbio.2014.07.021

50 Zhang, G., Fu, P., Wang, L. & Hu, M. Molecular spectroscopic studies of farrerol interaction with calf thymus DNA. *J. Agric. Food Chem.* **59**, 8944-8952 (2011). https://doi.org:10.1021/jf2019006

51 Eriksson, M. & Norden, B. Linear and circular dichroism of drug-nucleic acid complexes. *Methods Enzymol.* **340**, 68-98 (2001). https://doi.org:10.1016/s0076-6879(01)40418-6

52 Ivanov, V. I., Minchenkova, L. E., Schyolkina, A. K. & Poletayev, A. I. Different conformations of double-stranded nucleic acid in solution as revealed by circular dichroism. *Biopolymers* **12**, 89-110 (1973). https://doi.org:10.1002/bip.1973.360120109

53 Agarwal, S., Jangir, D. K. & Mehrotra, R. Spectroscopic studies of the effects of anticancer drug mitoxantrone interaction with calf-thymus DNA. *J. Photochem. Photobiol. B, Biol.* **120**, 177-182 (2013). https://doi.org:10.1016/j.jphotobiol.2012.11.001

54 Garbett, N. C., Ragazzon, P. A. & Chaires, J. B. Circular dichroism to determine binding mode and affinity of ligand-DNA interactions. *Nature Prot.* **2**, 3166-3172 (2007). https://doi.org:10.1038/nprot.2007.475

55 Searle, M. S. NMR studies of drug-DNA interactions. *Prog. NMR Spectrosc.* **25**, 403-480 (1993).

56 Swenberg, C. E., Carberry, S. E. & Geacintov, N. E. Linear dichroism characteristics of ethidium-and proflavine-supercoiled DNA complexes. *Biopolymers* **29**, 1735-1744 (1990). https://doi.org:10.1002/bip.360291406

57 Rehman, S. U., Sarwar, T., Husain, M. A., Ishqi, H. M. & Tabish, M. Studying non-covalent drug-DNA interactions. *Arch. Biochem. Biophys.* **576**, 49-60 (2015). https://doi.org:10.1016/j.abb.2015.03.024

58 Volker, J., Blake, R. D., Delcourt, S. G. & Breslauer, K. J. High-resolution calorimetric and optical melting profiles of DNA plasmids: resolving contributions from intrinsic melting domains and specifically designed inserts. *Biopolymers* **50**, 303-318 (1999). https://doi.org:10.1002/(SICI)1097-0282(199909)50:3<303::AID-BIP6>3.0.CO;2-U

59 Wing, R. *et al.* Crystal structure analysis of a complete turn of B-DNA. *Nature* **287**, 755-758 (1980). https://doi.org:10.1038/287755a0

60 Unione, L., Galante, S., Díaz, D., Cañada, F. J. & Jiménez-Barbero, J. NMR and molecular recognition. The application of ligand-based NMR methods to monitor molecular interactions. *MedChemComm* **5**, 1280-1289 (2014). https://doi.org:10.1039/C4MD00138A

61 Bauduin, P. *et al.* A theta-shaped amphiphilic cobaltabisdicarbollide anion: transition from monolayer vesicles to micelles. *Angew. Chem. Int. Ed.* **50**, 5298-5300 (2011). https://doi.org:10.1002/anie.201100410

62 Hendry, L. B., Mahesh, V. B., Bransome, E. D., Jr. & Ewing, D. E. Small molecule intercalation with double stranded DNA: Implications for normal gene regulation and for predicting the biological efficacy and genotoxicity of drugs and other chemicals. *Mutat. Res.* **623**, 53-71 (2007). https://doi.org:10.1016/j.mrfmmm.2007.03.009

63 Shi, J. H., Liu, T. T., Jiang, M., Chen, J. & Wang, Q. Characterization of interaction of calf thymus DNA with gefitinib: Spectroscopic methods and molecular docking. *J. Photochem. Photobiol. B, Biol.* **147**, 47-55 (2015). https://doi.org:10.1016/j.jphotobiol.2015.03.005

64 Taylor, R. & Kennard, O. Crystallographic evidence for the existence of C-H...O, C-H...N, and C-H...C1 hydrogen-bonds. *J. Am. Chem. Soc.* **104**, 5063-5070 (1982). https://doi.org:Doi 10.1021/Ja00383a012

65 Olejniczak, A. B., Nawrot, B. & Lesnikowski, Z. J. DNA Modified with boron-metal cluster complexes $[M(C_2B_9H_{11})_2]$–Synthesis, properties, and applications. *Int. J. Mol. Sci.* **19** (2018). https://doi.org:10.3390/Ijms19113501

66 Mitrea, D. M., Mittasch, M., Gomes, B. F., Klein, I. A. & Murcko, M. A. Modulating biomolecular condensates: A novel approach to drug discovery. *Nat. Rev. Drug Discov.* **21**, 841-862 (2022). https://doi.org:10.1038/s41573-022-00505-4

67 Bushweller, J. H. Targeting transcription factors in cancer - from undruggable to reality. *Nat. Rev. Cancer* **19**, 611-624 (2019). https://doi.org:10.1038/s41568-019-0196-7

68 Radaeva, M., Ton, A. T., Hsing, M., Ban, F. & Cherkasov, A. Drugging the 'undruggable'. Therapeutic targeting of protein-DNA interactions with the use of computer-aided drug discovery methods. *Drug Discov. Today* **26**, 2660-2679 (2021). https://doi.org:10.1016/j.drudis.2021.07.018

69 An, H. J. & Jin, B. Prospects of nanoparticle-DNA binding and its implications in medical biotechnology. *Biotechnol. Adv.* **30**, 1721-1732 (2012). https://doi.org:10.1016/j.biotechadv.2012.03.007

TOC